BMC Gastroenterology

RESEARCH

Open Access

Correlation analyses of ultrasonographic and histopathological characteristics of porta hepatis lymph nodes in biliary atresia

Zhen Huang[1†], Wen Ling[2†], Guorong Lyu[3,4], Shuxia Xu[1], Fengying Ye[2], Yifan Fang[5], Zongjie Weng[2*] and Qiumei Wu[2*]

Abstract

Background To perform correlation analyses between the ultrasonographic characteristics of porta hepatis lymph nodes (PHLNs) and the pathological features of PHLNs and the liver in biliary atresia (BA).

Methods We analyzed the clinical ultrasonographic characteristics of PHLNs in 27 patients with BA, along with specific pathological features, including pathological size, the number of bile granules, the number of germinal centers, the proportion of lymphocytes, and the analysis of liver biopsy specimens. A series of correlation analyses were then performed between ultrasonography data, pathological features, and prognosis.

Results The level of ultrasound echogenicity of PHLNs was positively correlated with the number of bile granules ($r=0.377$, $p=0.004$), while ultrasound and pathological size were also positively correlated with the number of germinal centers ($r=0.591$, $p=0.001$; $r=0.459$, $p=0.016$, respectively). No significant correlations were detected between the stage of liver fibrosis and pathological features or postoperative jaundice (all $p>0.05$). Different types of lymphocytes proliferating in the livers, and CD8 + cells were positively correlated with the pathological size of PHLNs ($r=0.390$, $p=0.045$; $r=0.424$, $p=0.028$, respectively), and the number of germinal centers($r=0.554$, $p=0.003$; $r=0.482$, $p=0.011$, respectively).The ultrasonographic and pathological size of PHLNs were only positively correlated with the serum levels of direct bilirubin($r=0.431$, $p=0.025$; $r=0.593$, $p=0.001$, respectively).Finally, the pathological size of PHLNs and the number of CD8 + cells in the liver were negatively correlated with the reduction of jaundice following Kasai portoenterostomy (KPE) surgery (r=-0.385, $p=0.047$; r=-0.567, $p=0.0411$; r=-0.002, $p=0.033$, respectively).

Conclusions Analyses demonstrated that the ultrasonographic features of PHLNs are significantly correlated with pathological features of PHLNs and the liver. In addition, the enlargement of PHLNs might represent a prognostic predictor following KPE surgery.

Keywords Biliary atresia, Porta hepatis lymph nodes, Sonographic features, Lymphocytes, Prognosis

†Zhen Huang and Wen Ling contributed equally to this work and share first authorship.

*Correspondence:
Zongjie Weng
wengzongjie1984@fjmu.edu.cn
Qiumei Wu
wqm0620@fjmu.edu.cn
[1]Department of Pathology, College of Clinical Medicine for Obstetrics & Gynecology and Pediatrics, Fujian Maternity and Child Health Hospital, Fujian Medical University, Fuzhou, China
[2]Department of Medical Ultrasonics, College of Clinical Medicine for Obstetrics & Gynecology and Pediatrics, Fujian Maternity and Child Health Hospital, Fujian Medical University, Fuzhou, China
[3]Department of Medical Ultrasonics, The Second Affiliated Hospital of Fujian Medical University, Quan zhou, China
[4]Department of Clinical Medicine, Quan zhou Medical College, Quan zhou, China
[5]Department of Pediatric Surgery, College of Clinical Medicine for Obstetrics & Gynecology and Pediatrics, Fujian Maternity and Child Health Hospital, Fujian Medical University, Fuzhou, China

Introduction

Surgeons often observe enlarged porta hepatis lymph nodes (PHLNs) in children when performing Kasai surgery for biliary atresia(BA) [1]. Previous studies have shown that the enlargement of PHLNs is related to the BA severity [2, 3]. Bove et al. [4] reported that lymphoid follicle hyperplasia was frequently detected in the PHLNs of children with BA, and that 53% of these nodes had germinal centers. The main factor contributing to the size of PHLNs known to be variable expansion of the inter follicular cortical lymphoid tissue in combination with reactive sinusoidal histiocytosis with a mixture of hematopoietic precursors and bile-stained macrophages. Consistent with the data reported by Bove et al. [4], our previous study also reported the detection of bile granules in enlarged PHLNs [5]. We hypothesized that macrophages phagocytize bile granules in the liver and then drain them into the PHLNs along with the lymph fluid, thus initiating an immune response, and causing reactive PHLNs hyperplasia. However, this hypothesis has yet to be fully confirmed. Furthermore, it has not been established whether there are correlations between microenvironmental changes, such as immune cell composition, the number of germinal centers, and the number of bile granules in the PHLNs of patients with BA, and the ultrasonographic characteristics of the PHLNs.

In BA, it is possible that the enlargement of PHLNs may be associated with liver fibrosis and the infiltration of inflammatory cells into the liver. Some studies have shown that the inflammatory response mediated by T cells in the liver plays a crucial role in the pathogenesis of BA [6, 7]. Pathologically, a large number of CD4 + and CD8 + T lymphocytes have been detected around the epithelium of the bile duct of the liver in patients with BA [6, 7]. CD4 + T cells regulate immune inflammation by secreting and activating inflammatory cells and inflammatory factors, thus accelerating liver inflammation and leading to BA [8]. Active CD8 + cytotoxic T cells have been shown to damage the epithelium of the bile duct and disrupt important physiological processes, such as the flow of bile [9].

In this study, we investigated the possible pathological mechanisms underlying PHLN enlargement by analyzing the correlations between ultrasonographic features and pathological features of PHLNs and the liver.

Methods

Patients

This study was approved by the Institutional Clinical Research Ethics Committee of Fujian Provincial Maternity and Children's Hospital in accordance with the Declaration of Helsinki, and written informed parental consent was waived due to the retrospective nature of the study. Between June 2019 to December 2021, we collated clinical data and pathological specimens of liver tissue and PHLNs from 27 patients with BA. The inclusion criteria were as follows: (1) pathological specimens needed to include PHLNs and liver tissues; (2) the patient had a complete set of laboratory examination data, including preoperative and postoperative follow-up clinical biochemical indicators. As a control group, we acquired samples of liver tissues from 15 patients with choledochal cysts.

Prognosis was judged by assessing whether jaundice disappeared (a total bilirubin level < 34.2μmol/L) three months after receiving the Kasai operation [10–13].

Ultrasonography techniques

All patients underwent abdominal ultrasound (US) scanning which was performed by two operators with more than 10 years of experience in pediatric US. The operators utilized a Voluson E8 scanner (GE Medical Systems) incorporating a 4–8 MHz curvilinear transducer and an 11-MHz linear array transducer. First, high-frequency transducers (> 10 MHz) were used to detect PHLNs. PHLNs were detected at the porta hepatis, in front of the main portal vein, and around the hepatoduodenal ligament. The maximal length and width of the PHLNs were measured and the number, shape, and echogenicity of the PHLNs were recorded. The size of the PHLNs was evaluated by calculating the cross-sectional area (area = maximum length × maximum width). PHLNs shape was categorized as regular (including circular or elliptical nodes) or irregular. Hyperechogenicity was defined when the ultrasonic echogenicity of the PHLNs was higher than that of the liver; in contrast, hypoechogenicity was defined when the ultrasonic echogenicity of the PHLNs was lower than that of the liver. If the patient had more than one detectable PHLNs, only the largest node was used for data analysis.

Histological and immunohistochemical staining

The PHLNs of all specimens were cut along the maximum diameter, and the maximal length and width were measured. The width was perpendicular to the maximal length, and the largest cross-sectional area was defined as the maximal length× the maximal width. If a patient had more than one detectable PHLNs, then only the largest node was selected for data analysis.

We used microscopy to observe and count the number of bile granules in sections of PHLNs. In this study, bile granules refer to bile pigment deposition particles observed in PHLN by hematoxylin-eosin (HE) staining, which were usually located in phagocytes and were about 1–5 μm in diameter. Macrophages were confirmed by staining with CD68 antibody (Table S1), and bile-stained macrophages were defined as cells showing both CD68 positivity and bile pigment deposition. The number of

bile granules were classified into three grades: grade 0 (no bile granules), grade 1+ (1–2 bile granules), grade 2+ (3–10bile granules), and grade 3+ (> 10bile granules).

Formalin-fixed and paraffin-embedded PHLNs were routinely sectioned and stained with antibodies against BCL-6, CD21, CD3, CD20, CD4, CD8 (Table S1). The number of germinal centers in PHLNs was quantitatively determined by immunohistochemical (IHC) staining of BCL-6 and CD21, and the number of different types of lymphocytes were semi-quantified according to the percentage of positive cells as a proportion of the total number of cells (including all positive and negative cells).

Formalin-fixed and paraffin-embedded liver samples were routinely sectioned and stained with Masson trichrome (Fuzhou Maxnew Biotech Co., Ltd.)and stained with CD3, CD20, CD4, and CD8 (Table S1).The staging of fibrosis in liver samples from patients with BA, and choledochal cysts, was evaluated according to Scheuer's fibrosis staging criteria [14]. Five hepatic lobules and portal area images (400×,3.60 × 2.97mm^2) were randomly acquired from each liver sample under 400× magnification (Leica microscope with a DFC450 camera), and the number of different types of lymphocytes were quantified in each field-of-view. The mean value was determined as the density of each positive cell when applying specific exclusion criteria, as follows: (1) the presence of other positive cells, such as interstitial cells and histiocytes; (2) perivascular lymphocytes; and (3) lymphocytes in lymphoid follicles [15, 16].

Statistical analysis

All statistical analyses were performed with SPSS version 20.0statistical software. The Shapiro-Wilk test was used to test whether quantitative data conformed to the normal distribution. Pearson's correlation or Spearman's rank correlation was used to analyze the correlations between quantitative variables or between quantitative variables and rank variables. Point-biserial analysis was used to analyze the correlations between two classification variables and quantitative variables. Kendall's Tau-b analysis was used to analyze the correlation between rank variables while Rank-biserial analysis was used to analyze the correlations between binary variables and rank variables. Fisher's exact probability method was used to analyze the correlations between unordered categorical variables. The t-test or Mann-Whitney U test was used to analyze the differences in quantitative variables between the choledochal cyst group (the control group) and the BA group. The c2 test or Fisher's exact probability method was used to compare the distribution of categorical variables between the choledochal cyst group and the BA group. Statistically significant differences were defined as those with p values < 0.05.

Results

Ultrasonographic features

The maximal area of PHLNs on US images taken from 27 patients with BA ranged from 59.5 to 296mm^2, with a median and interquartile range of 80.8 (68–131.3) mm^2. In total,24 patients (88.9%,24/27) had more than two PHLNs, and three patients (11.1%,3/27) had only one PHLN. Nine patients (33.3%,9/27) had PHLNs that were round while 18 patients (66.7%,18/27) had PHLNs that were irregular. The boundaries of all PHLNs were clear (100%,27/27); five patients (18.5%,5/27) were hypoechoic (Fig. 1A) and 22 patients (81.5%,22/27) were hyperechoic (Fig. 1B).

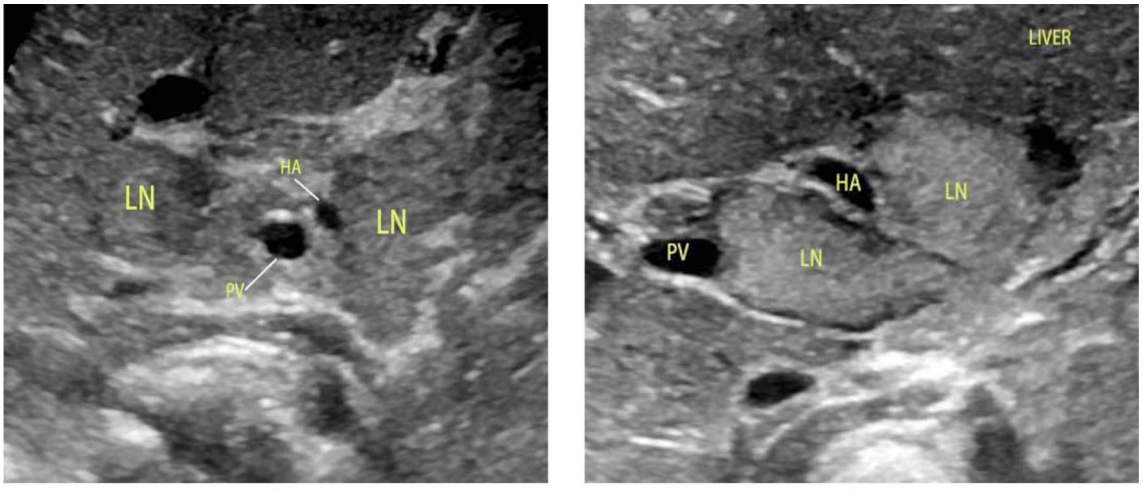

Fig. 1 Ultrasonic features of PHLNs in BA. (**A**) Male, 45 days: there were two PHLNs around the main portal vein in the hilar area, showing moderate and low echogenicity. (**B**) Male, 35days: there were two PHLNs around the main portal vein in the hilar area, and echogenicity was obviously enhanced. PHLN, porta hepatis lymph node; BA, biliary atresia

Clinical-pathological features

A total of 42 patients were included in this study, including 27 patients with BA and 15 patients with choledochal cysts (the control group). There were significant differences between the two groups in terms of gender and age ($p = 0.044$, $p = 0.0432$, respectively) (Table S2). Serum levels of direct bilirubin (DBIL), indirect bilirubin (IBIL), alanine aminotransferase (ALT), aspartate aminotransferase (AST) and gamma-glutamyl transpeptidase (GGT) in the BA group were significantly higher in the BA group than in the choledochal cyst group ($p < 0.001$ for all) (Table S2).

PHLNs of all 27 patients with BA were detected (Fig. 2A). The pathological size of the LNs ranged from 13.46 to 190.59mm^2, with a median of 67.75 (39.61–103.59) mm^2 (Table S3). Different degrees of lymphoid follicle hyperplasia were observed (Fig. 2B) (Table S3). Germinal centers were detected in 25 patients (25/27, 92.59%) (Fig. 2C). In addition, different numbers of bile granules were observed (Fig. 2D); nine patients were grade1+ (9/27, 33.33%), seven patients were grade2+ (7/27, 25.93%), and 11 patients were grade3+ (11/27,40.74%) (Table S3).

The pathological area of PHLNs was positively correlated with the number of germinal centers ($r = 0.591$, $p = 0.001$) (Table 1). There was no significant correlation between the number of bile granules and germinal centers in PHLNs in patients with BA ($p > 0.05$) (Table 1). The pathological size of PHLNs in BA, and the number of germinal centers and bile granules, were not significantly correlated with the proportions of different lymphocytes($p > 0.05$ for all) (Table 1).

Correlations between ultrasonographic features and pathological features

Correlation analysis between ultrasonographic features and the pathological features of PHLNs in patients with BA showed that the level of ultrasonic echogenicity was positively correlated with the number of bile granules ($r = 0.377$, $p = 0.004$, Table 2). The correlation between pathological size and the number of germinal centers was not statistically significant ($p > 0.05$, Table 2). The

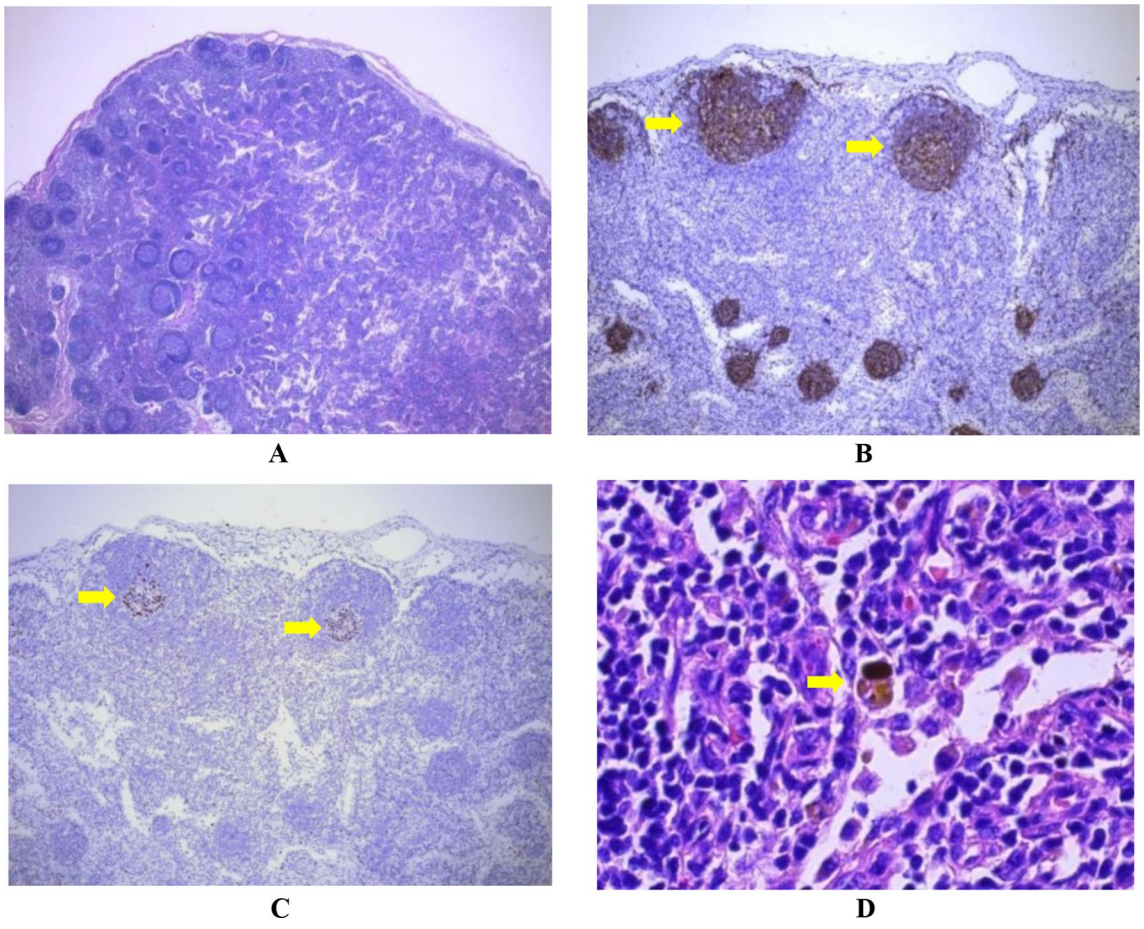

Fig. 2 PHLNs. (**A**) PHLNs were stained with HE. (**B**) CD21 staining of PHLNs and the follicular dendritic network of lymphatic follicle germinal centers were positive (IHC,×100). (**C**) BCL-6 staining in PHLNs showing positive germinal centers in lymph follicles (IHC, ×100). (**D**) 1–2bile granules (grade 1+) were observed by microscopy across an entire section of PHLNs (HE, ×400). PHLN, porta hepatis lymph node

Table 1 Correlation analyses of the pathological features of PHLNs in the BA group ($N=27$)

	Bile granules quantity grading	Germinal center quantity	CD3 + T cell ratio	CD20 + B cell ratio	CD4 + T cell ratio	CD8 + T cell ratio
Pathological size (mm^2)	0.247 (0.213)	0.591 (0.001)	0.0288 (0.887)	-0.184 (0.357)	-0.015 (0.941)	0.078 (0.697)
Germinal centers	0.133 (0.508)	1.000	0.068 (0.735)	0.026 (0.899)	-0.244 (0.220)	0.092 (0.649)
Grading of the number of bile granules	1.000	0.133 (0.508)	0.203 (0.245)	-0.314 (0.068)	0.294 (0.108)	0.265 (0.154)

p value is given in brackets

PHLN, porta hepatis lymph node; BA, biliary atresia

Table 2 Relationship between ultrasonographic features and the pathological features of PHLNs in the BA group

	Ultrasound echogenicity		Ultrasound area	
	Correlation coefficient	*P* value	Correlation coefficient	*P* value
Pathological size (mm^2)	0.079	0.697	0.317	0.108
Number of germinal centers	0.158	0.432	0.459	0.016
Grading of the number of bile granules	0.377	0.004	0.354	0.070

PHLN, porta hepatis lymph node; BA, biliary atresia

ultrasonic size was positively correlated with the number of germinal centers ($r=0.459$, $p=0.016$, Table 2). However, there was no significant correlation between pathological size and the number of bile granules($p>0.05$ for all, Table 2).

Correlations between the pathological features of PHLNs and pathological features in the liver

Analysis showed that the stages of liver fibrosis in the27 BA patients ranged from 2 to 4 (Table S4). No correlations were detected between pathological features and the stage of liver fibrosis ($p>0.05$ for all, Table S5).

Different degrees of lymphocyte infiltration were observed in the hepatic lobule and portal area of the liver in the BA group (Fig. 3A and B) (Table S6). Furthermore, more CD3 + T lymphocytes, CD20 + B lymphocytes and CD4 + T lymphocytes were distributed in the portal area than in the hepatic lobules ($p<0.001$, Table S6). Correlation analysis showed that the pathological size of the PHLNs was correlated with the number of CD8 + T cells in the hepatic lobule ($r=0.390$, $P=0.045$) (Fig. 3C), and the portal area ($r=0.424$, $p=0.028$) (Fig. 3D) (Table 3). The number of germinal centers was positively correlated with the proportions of CD3 + T cells and CD8 + T cells in the hepatic lobules and portal area ($p<0.05$ for all). However, there was no significant correlation between the number of germinal centers and the proportions of CD20 + B and CD4 + T lymphocytes ($p>0.05$ for all, Table 3). There was no significant correlation between the number of bile granules in PHLNs and the proportion of lymphocytes in the liver ($p>0.05$ for all, Table 3).

Compared with the choledochal cyst (control) group, the stage of liver fibrosis in the BA group mainly ranged from stage 3 to 4 (77.78%); this compared to stages 0 and 1 in the choledochal cyst group (accounting for 80%) (Table S7). The number of lymphocytes in the BA group was also significantly higher than that in the choledochal cyst group (Table S7).

Correlations between ultrasonographic, clinical-pathological features, and prognosis

The ultrasound and pathological size of PHLNs in patients with BA were only positively correlated with the serum level of direct bilirubin (Table S8). There was no significant correlation between ultrasound echogenicity, the number of bile granules, the number of germinal centers, and each clinical index (Table S8).

In this study, jaundice disappeared in 14 patients with BA (51.9%). For the rest 13 patients (48.1%), jaundice persisted for three months after KPE surgery. The pathological size of PHLNs in patients with BA, and the number of CD8 + T cells in the hepatic lobule and portal area, were negatively correlated with the reduction of jaundice three months after KPE surgery. There was no significant correlation between the other types of lymphocytes in the liver ($p>0.05$ for all, Tables 4 and 5) and ultrasound size and echogenicity, the number of bile granules, the number of germinal centers, and the stage of liver fibrosis.

Discussion

In a previous study, Bove et al. [4] reported that PHLNs in patients with BA were significantly larger than those incidentally found at the junction of the hepatic duct and cystic duct around the proximal biliary remnant at or near the lesions, thus suggesting an important relationship between PHLNs and BA. Furthermore, these authors also found that lymphoid follicle hyperplasia was often observed in the enlarged PHLNs; the mean number of germinal centers was $3.2/mm^2$, and the number of germinal centers correlated with the area and increased with age [4]. The germinal center is a place where B cells differentiate and represents the immune response of human

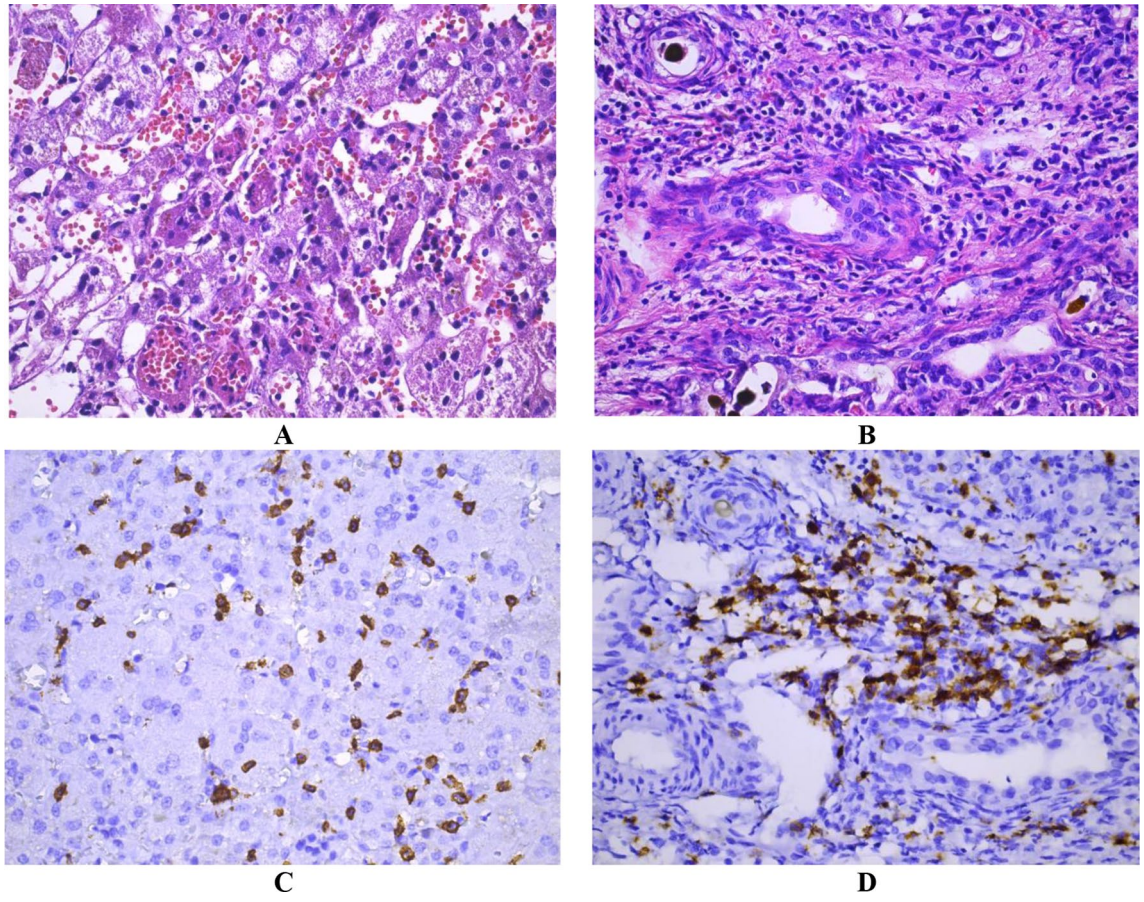

Fig. 3 Lymphocyte infiltration in the liver. (**A**) Scattered lymphocyte infiltration in the hepatic lobule of a liver in BA group (HE, ×400). (**B**) A large number of lymphocytes infiltrating the portal area of the liver in the BA group (HE, ×400). (**C**) Immunohistochemical staining of CD8 + T lymphocytes in the hepatic lobule of liver in the BA group (IHC, ×400). (**D**) Immunohistochemical staining of CD8 + T lymphocytes in the hepatic portal area of the BA group (IHC,×400)

Table 3 Correlation analyses between the pathological features of PHLNs and liver lymphocytes in the BA group

	CD3 + T cells		CD20 + B cells		CD4 + T cells		CD8 + T cells	
	Hepatic lobule	Hepatic portal area	Hepatic lobule	Hepatic portal area	Hepatic lobule	Hepatic portal area	Hepatic lobule	Hepatic portal area
Pathological size(mm^2)	0.336 (0.087)	0.173 (0.389)	-0.194 (0.332)	-0.196 (0.327)	0.208 (0.297)	0.049 (0.808)	0.390 (0.045)	0.424 (0.028)
Bile granules	-0.105 (0.603)	-0.354 (0.070)	-0.183 (0.362)	-0.352 (0.072)	0.089 (0.658)	-0.029 (0.886)	−0.269 (0.175)	-0.354 (0.070)
Germinal centers	0.480 (0.011)	0.490 (0.010)	0.187 (0.351)	-0.042 (0.836)	0.297 (0.132)	0.261 (0.189)	0.554 (0.003)	0.482 (0.011)

p value is given in brackets

PHLN, porta hepatis lymph node; BA, biliary atresia

LNs to antigenic stimulation. This process needs to occur one to two weeks after exposure to an antigen, and has been observed in perinatal infant autopsy [17]. In addition, bile-stained macrophages are also one of the main factors contributing to the enlargement of PHLNs [4]. Consistent with the study by Bove et al. [4], our present data show that more than 90% of PHLNs in patients with BA produced a variable number of germinal centers; in addition, bile-stained macrophages were observed. Bile-stained macrophages (confirmed by CD68 IHC) may contribute to PHLN enlargement in part by phagocytosis of bile pigment, but their number was not significantly correlated with hepatic lymphocyte infiltration, suggesting that their immune activation role was limited. Instead, PHLN swelling was more likely driven by germinal center activation. The phagocytosis of macrophages

Table 4 Ultrasonic features of PHLNs in the BA group, the pathological features of PHLNs and their correlation with prognosis

	Prognosis	*P* value
	Correlation coefficient	
Ultrasound size (mm^2)	0.174	0.385
Ultrasound echogenicity[a]	/	0.370
Pathological size (mm^2)	-0.385	0.047
Germinal centers	0.236	0.237
Bile granules	-0.126	0.452

a: Fisher's exact probability method was used to analyze the correlation between unordered categorical variables

PHLN, porta hepatis lymph node; BA, biliary atresia

Table 5 Correlation analyses between the pathological features of the liver and the prognosis of BA

		Prognosis	
		Correlation coefficient	*P* value
Liver fibrosis stage[a]		/	1.000
CD3 + T cells	Hepatic lobule area	0.313	0.112
	Hepatic portal area	0.284	0.151
CD20 + T cells	Hepatic lobule area	0.110	0.584
	Hepatic portal area	-0.042	0.835
CD4 + T cells	Hepatic lobule area	0.344	0.079
	Hepatic portal area	0.376	0.053
CD8 + T cells	Hepatic lobule	-0.567	0.002
	Hepatic portal area	-0.411	0.033

a: Fisher's exact probability method was used to analyze the correlation between unordered categorical variables

BA, biliary atresia

may only be a passive response to cholestasis, rather than a core mechanism of BA inflammation. The relationship between bile granules in PHLNs and immune response PHLNs still needs to be further verified by animal experiments.

Hepatic fibrosis is an important pathological manifestation of BA. Hepatic fibrosis can cause bile drainage disorder, thus resulting in reduced intrahepatic bile discharge, thereby affecting the drainage of PHLNs. This study did not find a statistically significant correlation between PHLNs enlargement and the degree of liver fibrosis. However, the increase in the area and number of germinal centers in PHLNs is associated with CD8 + in the liver. The infiltration of T lymphocytes indicates that PHLNs may participate in the pathological process of BA through immune regulation. Its specific relationship with liver fibrosis needs further study. Following biliary obstruction, immune-mediated biliary injury persisted regardless of the restoration of bile flow after KPE surgery, thus suggesting that bile extravasation cannot be the sole explanation for liver injury [18]. It is still unclear whether the obvious inflammatory reaction in and outside of the liver in patients with BA is a secondary reaction to cholestasis and biliary obstruction or the root cause of bile duct destruction and liver fibrosis [19].

The inflammatory response mediated by T cells in the livers of patients with BA plays a crucial role in disease pathogenesis. Previous studies have shown that hepatic inflammatory cells are mainly infiltrated by CD4 + and CD8 + T cells [6, 7], especially CD8 + T lymphocytes. In this study, we detected obvious infiltration of CD4 + T cells and CD8 + T cells in the hepatic lobule and portal area; these observations do not concur with those of Davenport et al. and Mack et al., who previously reported that CD4 + T cells were the most common form of lymphocytes [19–21]. In a previous study, involving a rotavirus-infected mouse model of BA, researchers found that the increased infiltration of CD4 + T and CD8 + T cells could trigger inflammation and lead to biliary epithelial damage [22–24]. Shivakumar et al. [9] found that the reduction of CD4 + T cells did not change the progression of inflammatory injury and bile duct obstruction, and that the loss of CD8 + T cells significantly inhibited bile duct damage in an animal model, thus indicating that bile duct damage was mainly due to CD8 + T cells. In the present study, we detected larger areas and higher numbers of germinal centers in PHLNs, along with a high number of CD8 + T lymphocytes in the livers of patients with BA, thus suggesting that the severity of liver bile duct injury could be reflected by the size of PHLNs.

In this study, we did not identify a significant correlation between PHLNs and B lymphocytes in the liver. At present, the specific role of B lymphocytes in BA remains unclear. B lymphocytes mainly play an auxiliary role in BA and do not only activate T cells by secreting cytokines [25]; they also activate T cells by secreting their own antigens to promote T cell activation and pathogenic function [26–28]. The depletion of B lymphocytes in BA has been associated with impaired effector T cell activation and protection from biliary injury, further confirming the helper role played by B lymphocyte [28]. The specific relationship between PHLNs and B lymphocytes in the liver has yet to be fully elucidated.

In the present study, the stage of fibrosis and the degree of inflammatory infiltration in the BA group were significantly higher than those in the choledochal cyst (control) group, thus indicating that BA was a serious inflammatory disease that often causes damage to the liver and bile duct. In an animal model of BA, CD8 + T lymphocytes in the liver can be activated in the early stage of the disease, thus leading to biliary epithelial damage; this process can also induce the expression of osteopontin in the biliary tract and biliary stromal cells to initiate biliary fibrosis [29]. Previous studies have shown that osteopontin is a pro-fibrotic cytokine and a driver that bridges fibrosis with pleiotropic effects on cell proliferation, migration, inflammation and fibrosis [30–32]. In

an experimental model of cholestasis, the expression of osteopontin has been shown to be associated with the stage of biliary fibrosis in infants with BA by regulating the interaction of TGF-β with hepatic stellate cells and myofibroblasts secreting collagen 1 [33]. In the presents study, the number of various types of T lymphocytes in the livers of patients in the BA group were significantly higher than those of the control group, thus resulting in differing severities of liver fibrosis; these findings concur with those reported by previous studies [6, 7].

It has been reported that the degree of enlargement in PHLNs is related to the progression of BA [2, 3]. Consistent with previous studies, our analyses showed that the pathological size of the PHLNs was negatively correlated with jaundice following KPE surgery; in other words, the larger the size, the worse the prognosis. This may be because the size of the PHLNs reflects the severity of cholestasis (increased phagocytosis in bile granules) and the degree of inflammation in the hepatobiliary system (an increased number of germinal centers). However, in the present study, there was no significant correlation between the ultrasonographic size of the PHLNs area and the prognosis of patients following KPE surgery. This lack of significance may be due to the fact that this study was retrospective, because the number of BA specimens was small, and because the PHLNs displayed by ultrasound were not completely consistent with those obtained during surgery. In contrast to the findings reported by Ahmed et al. and Derkow et al. [34, 35], we found that a greater number of CD8 + T lymphocytes in the livers of patients with BA, the worse the effect of jaundice reduction three months after surgery. Our findings also differ from those reported by Zhang et al. who reported that increased numbers of CD4 + T cells were associated with a poor prognosis [36]. The results are inconsistent which may be related to the method used to determine the number of lymphocytes; some authors used semi-quantitative methods for counting, while others use quantitative counting methods.

The study has some limitations that need to be considered. First, we only studied the pathological features of PHLNs in BA; we did not conduct pathological analysis on the potential small PHLNs of choledochal cysts. Second, we only analyzed 27 patients; this could have exerted impact on statistical validity. Finally, we did not perform animal experiments to investigate the specific pathological mechanisms that might underlie PHLNs enlargement. These limitations need to addressed in future research.

Conclusions

In conclusion, our analyses found that the ultrasonographic features of PHLNs in BA are correlated with the pathological features of PHLNs and the liver. In addition, the enlargement of PHLNs might play a role in predicting prognosis following KPE surgery.

Abbreviations

PHLN	Porta hepatis lymph node
LN	Lymph node
BA	Biliary atresia
KPE	Kasai portoenterostomy
HE	Hematoxylin and eosin
IHC	Immunohistochemical
DBIL	Serum direct bilirubin
IBIL	Indirect bilirubin
ALT	Alanine aminotransferase
AST	Aspartate aminotransferase
GGT	Gamma-glutamyl transpeptidase

Supplementary Information

The online version contains supplementary material available at https://doi.org/10.1186/s12876-025-03972-2.

Supplementary Material 1

Acknowledgements

We deeply thank Hong Ma for providing insightful discussions during the preparation of the manuscript and without whom this work would not have been possible.

Author contributions

ZW: Study concept and design, critical revision of the manuscript for important intellectual content, administrative, technical, or material support, study supervision; QW: Study concept and design, critical revision of the manuscript for important intellectual content, administrative, technical, or material support; ZH: acquisition of data, drafting of the manuscript, critical revision of the manuscript for important intellectual content; WL: acquisition of data, drafting of the manuscript, critical revision of the manuscript for important intellectual content; GL: analysis and interpretation of data; SX: analysis and interpretation of data, administrative, technical, or material support; FY: analysis and interpretation of data; YF: analysis and interpretation of data. All authors have made a significant contribution to this study and have approved the final manuscript.

Funding

The work was supported in part by a grant from the Fujian Provincial Health Technology Project [grant number 2020GGB015 to WZJ].

Data availability

The datasets used and/or analysed during the current study are available from the corresponding author on reasonable request.

Declarations

Ethics approval and consent to participate

This study was approved by the Institutional Review Board and Ethics Committee of the Fujian Provincial Maternity and Child Health Hospital in accordance with the Declaration of Helsinki. written informed parental consent was waived due to the retrospective nature of the study.

Consent for publication

Not applicable.

Competing interests

The authors declare no competing interests.

Received: 2 December 2024 / Accepted: 5 May 2025
Published online: 23 May 2025

References

1. Muraji T, Suskind DL, Irie N. Biliary Atresia: A new immunological insight into etiopathogenesis. Expert Rev Gastroenterol Hepatol. 2009;3(6):599–606. https://doi.org/10.1586/egh.09.61.
2. Sakamoto N, Muraji T, Ohtani H, Masumoto K. The accumulation of regulatory T cells in the hepatic hilar lymph nodes in biliary Atresia. Surg Today. 2017;47:1282–6. https://doi.org/10.1007/s00595-017-1502-1.
3. Engelmann C, Maelzer M, Kreyenberg H. Absence of maternal microchimerism in loco-regional lymphnodes of children with biliary Atresia. J Pediatr Gastroenterol Nutr. 2015;62:804–7. https://doi.org/10.1097/MPG.0000000000001093.
4. Bove K, Sheridan R, Tengfei L, Anders R, Chung C, Cummings O, et al. Hepatic hilar lymph node reactivity at Kasai portoenterostomy for biliary Atresia. Pediatr Dev Pathol. 2017;21:29–40. https://doi.org/10.1177/1093526617707851.
5. Weng Z, Luyao Z, Wu Q, Zhou W, Ma H, Fang Y, et al. Enlarged hepatic hilar lymph node: an additional ultrasonographic feature that May be helpful in the diagnosis of biliary Atresia. Eur Radiol. 2019;29:6699–707. https://doi.org/10.1007/s00330-019-06339-w.
6. Jiang H, Gao P, Chen H, Zhong Z, Shu M, Zhang Z, et al. The prognostic value of CD8 + and CD45RO + T cells infiltration and beclin1 expression levels for early postoperative cholangitis of biliary Atresia patients after Kasai operation. J Korean Med Sci. 2018;33:e198. https://doi.org/10.3346/jkms.2018.33.e198.
7. Liu L, Liu J, Luo J, Yang R, Li K, Zhu Z, et al. Dysregulated proportion of intrahepatic Treg cells and Th17 along with CD8 + T lymphocytes drives disease progression after Kasai biliary Atresia surgery. Chin J Hepatol. 2021;29:150–5. https://doi.org/10.3760/cma.j.cn501113-20200216-00048.
8. Zhang K, Chen Y, Zheng Z, Tang C, Zhu D, Xia X, et al. Relationship between the expression levels of CD4 + T cells, IL-6, IL-8 and IL-33 in the liver of biliary Atresia and postoperative cholangitis, operative age and early jaundice clearance. Pediatr Surg Int. 2022;38:1939–47. https://doi.org/10.1007/s00383-022-05258-0.
9. Shivakumar P, Sabla G, Mohanty S, McNeal M, Ward R, Stringer K, et al. Effector role of neonatal hepatic CD8 + lymphocytes in epithelial injury and autoimmunity in experimental biliary Atresia. Gastroenterology. 2007;133:268–77. https://doi.org/10.1053/j.gastro.2007.04.031.
10. Ramos-Gonzalez G, Elisofon S, Dee E, Staffa S, Medford S, Lillehei C, et al. Predictors of need for liver transplantation in children undergoing Hepatoportoenterostomy for biliary Atresia. J Pediatr Surg. 2019;54:1127–31. https://doi.org/10.1016/j.jpedsurg.2019.02.051.
11. Nguyen AH, Pham Y, Vu G, Hà M, Hoang T, Holterman A. Biliary Atresia liver histopathological determinants of early post-Kasai outcome. J Pediatr Surg. 2021;56:1169–73. https://doi.org/10.1016/j.jpedsurg.2021.03.039.
12. Sundaram S, Mack C, Feldman A, Sokol R. Biliary Atresia: indications and timing of liver transplantation and optimization of pre-transplant care. Liver Transpl. 2017;23:96–109. https://doi.org/10.1002/lt.24640.
13. Shneider B, Magee J, Karpen S, Rand E, Narkewicz M, Bass L, et al. Total serum bilirubin within 3 months of Hepatoportoenterostomy predicts short-term outcomes in biliary Atresia. J Pediatr. 2015;170:211–7. https://doi.org/10.1016/j.jpeds.2015.11.058.
14. Desmet VJ, Gerber M, Hoofnagle JH, Manns M, Scheuer PJ. Classification of chronic hepatitis: diagnosis, grading and staging. Hepatology. 1994;19(6):1513–20.
15. Liu K, Yang K, Wu B, Chen HN, Chen XL, Chen XZ, et al. Tumor-infiltrating immune cells are associated with prognosis of gastric cancer. Med (Baltim). 2015;94(39):e1631. https://doi.org/10.1097/MD.0000000000001631.
16. Kim KJ, Lee K, Cho HJ, Kim YH, Yang H, Kim W, et al. Prognostic implications of tumor-infiltrating FOXp3 + regulatory T cells and CD8 + cytotoxic T cells in microsatellite-unstable gastric cancers. Hum Pathol. 2013;45:285–93. https://doi.org/10.1016/j.humpath.2013.09.004.
17. Coots A, Donnelly B, Mohanty S, McNeal M, Sestak K, Tiao G. Rotavirus infection of human cholangiocytes parallels the murine model of biliary Atresia. J Surg Res. 2012;177:275–81. https://doi.org/10.1016/j.jss.2012.05.082.
18. Lampela H, Kosola S, Heikkilä P, Lohi J, Jalanko H, Pakarinen M. Native liver histology after successful portoenterostomy in biliary Atresia. J Clin Gastroenterol. 2013;48:721–8. https://doi.org/10.1097/MCG.0000000000000013.
19. Mack C, Tucker R, Sokol R, Karrer F, Kotzin B, Whitington P, et al. Biliary Atresia is associated with CD4 + Th1 cell–mediated portal tract inflammation. Pediatr Res. 2004;56:79–87. https://doi.org/10.1203/01.PDR.0000130480.51066.FB.
20. Davenport M, Gonde C, Redkar R, Koukoulis G, Tredger M, Mieli-Vergani G, et al. Immunohistochemistry of the liver and biliary tree in extrahepatic biliary Atresia. J Pediatr Surg. 2001;36:1017–25. https://doi.org/10.1053/jpsu.2001.24730.
21. Broomé U, Nemeth A, Hultcrantz R, Scheynius A. Different expression of HLA-DR and ICAM-1 in livers from patients with biliary Atresia and Baler's disease. J Hepatol. 1997;26:857–62. https://doi.org/10.1016/S0168-8278(97)80253-X.
22. Carvalho E, Liu C, Shivakumar P, Sabla G, Aronow B, Bezerra J. Analysis of the biliary transcriptome in experimental biliary Atresia. Gastroenterology. 2005;129:713–7. https://doi.org/10.1016/j.gastro.2005.05.052.
23. Leonhardt J, Stanulla M, Wasielewski R, Skokowa J, Kübler J, Ure B, et al. Gene expression profile of the infective murine model for biliary Atresia. Pediatr Surg Int. 2006;22:84–9. https://doi.org/10.1007/s00383-005-1589-0.
24. Mack C, Tucker R, Lu B, Sokol R, Fontenot A, Ueno Y, et al. Cellular and humoral autoimmunity directed at bile duct epithelia in murine biliary Atresia. Hepatology (Baltimore MD). 2006;44:1231–9. https://doi.org/10.1002/hep.21366.
25. Bednarek J, Traxinger B, Brigham D, Roach J, Orlicky D, Wang D, et al. Cytokine-producing B cells promote immune-mediated bile duct injury in murine biliary Atresia. Hepatology. 2017;68:1890–904. https://doi.org/10.1002/hep.30051.
26. Falcone M, Lee J, Patstone G, Yeung B, Sarvetnick N. B lymphocytes are crucial antigen-presenting cells in the pathogenic autoimmune response to GAD65 antigen in Nonobese diabetic mice. J Immunol. 1998;161:1163–8. https://doi.org/10.4049/jimmunol.161.3.1163.
27. Noorchashm H, Lieu YK, Noorchashm N, Rostami Y, Greeley SA, Schlachterman A, et al. I-A(g7)-mediated antigen presentation by B lymphocytes is critical in overcoming a checkpoint in T cell tolerance to islet beta cells of Nonobese diabetic mice. J Immunol. 1999;163:743–50.
28. Wong F, Wen L, Tang M, Ramanathan M, Visintin I, Daugherty J, et al. Investigation of the role of B-cells in type 1 diabetes in the NOD mouse. Diabetes. 2004;53:2581–7. https://doi.org/10.2337/diabetes.53.10.2581.
29. Taylor A, Carey A, Kudira R, Lages C, Shi T, Lam S, et al. Interleukin 2 promotes hepatic regulatory t cell responses and protects from biliary fibrosis in murine sclerosing cholangitis. Hepatology. 2018;68:1905–24. https://doi.org/10.1002/hep.30061.
30. Strazzabosco M, Fabris L, Albano E, Osteopontin. A new player in regulating hepatic ductular reaction and hepatic progenitor cell responses during chronic liver injury. Gut. 2014;63:1693–4. https://doi.org/10.1136/gutjnl-2014-307712.
31. Coombes J, Swiderska-Syn M, Dollé L, Reid D, Eksteen B, Claridge L, et al. Osteopontin neutralization abrogates the liver progenitor cell response and fibrogenesis in mice. Gut. 2014;64:1120–31. https://doi.org/10.1136/gutjnl-2013-306484.
32. Wang X, Lopategi A, Ge X, Lu Y, Kitamura N, Urtasun R, et al. Osteopontin induces ductular reaction contributing to liver fibrosis. Gut. 2014;63:1805–18. https://doi.org/10.1136/gutjnl-2013-306373.
33. Huang L, Wei MF, Feng JX. Abnormal activation of OPN inflammation pathway in livers of children with biliary Atresia and relationship to hepatic fibrosis. Eur J Pediatr Surg. 2008;18:224–9. https://doi.org/10.1055/s-2008-1038483.
34. Ahmed AF, Ohtani H, Nio M, Funaki N, Iwami D, Kumagai S, et al. In situ expression of fibrogenic growth factors and their receptors in biliary Atresia: comparison between early and late stages. J Pathol. 2000;192:73–80. https://doi.org/10.1002/1096-9896(2000)9999:9999%3C::AID-PATH657%3E3.0.CO;2-J.
35. Derkow K, Loddenkemper C, Mintern J, Kruse N, Klugewitz K, Berg T, et al. Differential priming of CD8 and CD4 T-Cells in animal models of autoimmune hepatitis and cholangitis. Hepatology. 2007;46:1155–65. https://doi.org/10.1002/hep.21796.
36. Zhang S, Goswami S, Ma J, Meng L, Wang Y, Zhu F, et al. CD4 + T cell subset profiling in biliary Atresia reveals ICOS– regulatory T cells as a favorable prognostic factor. Front Pediatr. 2019;7:279. https://doi.org/10.3389/fped.2019.00279.

Publisher's note